



Accepted Article

Title: Platinum(II) complexes of curcumin showing photocytotoxicity in visible light

Authors: Akhil Chakravarty; Koushambi Mitra; Srishti Gautam; Paturu Kondaiah

This manuscript has been accepted after peer review and the authors have elected to post their Accepted Article online prior to editing, proofing, and formal publication of the final Version of Record (VoR). This work is currently citable by using the Digital Object Identifier (DOI) given below. The VoR will be published online in Early View as soon as possible and may be different to this Accepted Article as a result of editing. Readers should obtain the VoR from the journal website shown below when it is published to ensure accuracy of information. The authors are responsible for the content of this Accepted Article.

To be cited as: Eur. J. Inorg. Chem. 10.1002/ejic.201601078

Link to VoR: <http://dx.doi.org/10.1002/ejic.201601078>

Platinum(II) complexes of curcumin showing photocytotoxicity in visible light

Koushambi Mitra,^[a] Srishti Gautam,^[b] Paturu Kondaiah*^[b] and Akhil R. Chakravarty*^[a]

Abstract: Three platinum(II) complexes of curcumin, [Pt(NH₃)₂(cur)](NO₃) (**1**), [Pt(en)(cur)](NO₃) (**2**) and [Pt(dach)(cur)](NO₃) (**3**) where Hcur is curcumin, en is ethylene diamine and dach is 1R,2R(-)-1,2-diamminocyclohexane were synthesized, characterized and their photocytotoxic properties explored. The acetylacetone (Hacac) analogue of **1**, [Pt(NH₃)₂(acac)]NO₃ (**4**) was prepared to investigate the role of photoactive curcumin. The crystal structure of [Pt(NH₃)₂(acac)]CF₃SO₃ (**4a**) revealed square planar geometry of the platinum(II) centre. Complexes **1-3** displayed intense absorption band at 450 nm ($\epsilon = 22500 \text{ M}^{-1} \text{ cm}^{-1}$). The curcumin in metal bound form showed improved stability in 10% DMSO-buffer solution at 37°C. The complexes released curcumin on irradiation with visible light (400-700 nm) as evident from the increment in emission intensity. The complexes formed Pt-DNA covalent adducts when treated with ct-DNA and exposed to light. The platinum-curcumin conjugates demonstrated photocytotoxicity in cancer cells giving IC₅₀ values of 15-45 μM (400-700 nm, 10 J cm⁻²) with no apparent activity in the dark (IC₅₀: > 200 μM). Cytoplasmic localization and ROS mediated apoptotic cell death in visible light was observed for the curcumin complexes.

Introduction

Platinum(II) complexes are the mainstay of cancer chemotherapy.^[1-3] Cisplatin, oxaliplatin and carboplatin are the clinically approved chemotherapeutic agents.^[4-6] Though highly efficacious, these anticancer agents suffer from dose-limiting adverse effects such as hepatotoxicity, nephrotoxicity, ototoxicity, reduction in platelet counts and myelosuppression.^[7,8] Another major disadvantage is the associated acquired or inherent drug resistance.^[2] Thus, chemical modifications of these drugs became essential which led to the development of a vast library of platinum based anticancer agents.^[9-12] These alterations were primarily made to reduce the chances of prior activation and to obtain controlled generation of active platinum(II) species capable of damaging DNA. Such attempts were made by

changing the leaving groups and modulating the ligand dissociation kinetics. In addition, inert platinum(IV) prodrugs are suitably designed for reduction to generate active species in intercellular environment in presence of glutathione or ascorbic acid.^[13-15] By tuning the axial ligands of these platinum(IV) complexes, targeted and improved antiproliferative properties in cancer cells were achieved.^[16-18] Recently, it was observed that Pt(IV) diazido complexes undergo photo-reduction in UVA or blue light to generate lethal cytotoxins such as platinum(II) DNA crosslinkers, reactive oxygen and nitrogen species.^[19-23] The photoactivated chemotherapy (PACT) emerged as one of the most selective strategies in which a prodrug on photo-triggered activation leads to selective destruction of tumor lesions.^[24-27]

The present work stems from our interest to develop platinum(II) complexes of curcumin where this dye in its enolic form can bind to the metal with a possibility to release it in a cellular medium on photoactivation. Curcumin, a polyphenolic chief constituent of *Curcuma* (Indian spice turmeric) gained immense therapeutic attention due to its remarkable antioxidant, anti-inflammatory, antiseptic, and anticancer properties.^[28-30] The excellent biocompatibility and reduced side effects exhibited by this molecule even at higher consumption levels are unique when compared to that of existing organic anticancer drug armamentarium.^[29] Curcumin with its *O,O*-donor binding sites could model oxaliplatin and carboplatin having the *O,O*-donor ligands. However, despite its having beneficial medicinal properties, unformulated curcumin failed to achieve clinical success due to hydrolytic instability in a biological medium followed by rapid clearance of the degraded products thus reducing its cellular accumulation.³¹ Another demerit of curcumin is its poor aqueous solubility. One of the many approaches to prevent the degradation of curcumin is its metallation in which the 1,3-diketone moiety in its enolic form acts as a bi-dentate *O,O*-donor ligand. Stable transition metal complexes of curcumin are well documented to show novel cytotoxic properties.^[32-35] Moreover, curcumin complexes were found to serve as potential photocytotoxic agents utilizing photosensitizing property of this dye.^[36]

The use of platinum anticancer agents and curcumin in adjunct or combination therapy has been previously reported.^[37] However, controlled delivery of curcumin and the platinum drug from a single prodrug is much more desired. With these motivations, we synthesized and communicated the photo-induced cytotoxicity of a platinum-curcumin conjugate, [Pt(NH₃)₂(cur)](NO₃) (**1**) where we demonstrated the photo-induced release of curcumin in visible light.^[36d] In this full report, we modulated the ammine ligand and evaluated a qualitative structure-activity relationship of their photocytotoxic profiles. Two more platinum(II) complexes of curcumin, viz. [Pt(en)(cur)](NO₃) (**2**) and [Pt(dach)(cur)](NO₃) (**3**) where Hcur is curcumin, en is ethylenediamine and dach is 1R,2R(-)-1,2-diaminocyclohexane,

[a] K. Mitra, A. R. Chakravarty*
Department of Inorganic and Physical Chemistry
Indian Institute of Science, Bangalore 560-012
E-mail: arc@ipc.iisc.ernet.in
<http://ipc.iisc.ac.in/arc.php>
[b] S. Gautam, P. Kondaiah*
Department of Molecular Reproduction, Development and Genetics
Indian Institute of Science, Bangalore 560-012
E-mail: paturu@mrdg.iisc.ernet.in
<http://mrdg.iisc.ernet.in/paturu-new/Home.htm>

Supporting information for this article is given via a link at the end of the document. ((Please delete this text if not appropriate))

were synthesized, characterized and their photocytotoxic properties studied. The acetylacetonate (Hacac) analogue of **1**, [Pt(NH₃)₂(acac)]NO₃ (**4**) was used as a control to investigate the role of the photoactive curcumin ligand (Figure 1).

Results and Discussion

Synthesis and general aspects

Complexes **1** and **4** were prepared by first replacing the chlorides of cisplatin by nitrates by using silver nitrate and then by reacting the yellow filtrate with one equivalent of either Hcur (for **1**) or Hacac (for **4**) in presence of a base to isolate the desired complexes (yield ~70%) (Scheme S1, the Supporting Information). Complexes **2** and **3** were prepared by using the corresponding amine substituted chloroplatinum(II), viz. [Pt(en)Cl₂] for **2** and [Pt(dach)Cl₂] for **3**, as the precursor complexes (Scheme S2, the Supporting Information). All the complexes were characterized from spectroscopic and analytical data (Table 1, Figures S1-S10, the Supporting Information). The molar conductance of the complexes **1-4** were found to be ~80 S cm² mol⁻¹ at room temperature in aq. DMF (1:1 v/v) suggesting their 1:1 electrolytic nature. The mass spectra of the complexes in methanol showed a maximum abundance of [M-NO₃]⁺ species (*m/z* = 596.13 for **1**, 622.15 for **2**, 677.20 for **3** and 328.25 for **4**). The isotopic distribution of the peak indicated the presence of platinum as well as the unipositive nature of the ionic fragments (Figures S1-S4, the Supporting Information). The ¹H NMR spectra of the complexes **1-3** recorded in d₄-methanol revealed peaks in the region 6.5-8.0 ppm which were assignable to the aromatic protons of the curcumin moiety. The gamma proton of the diketonate moiety was found at 5.8-5.9 ppm (Figures S5-S7, the Supporting Information). The same for free curcumin appeared at 6.0 ppm indicating that the coordination to platinum(II) centre resulted in an upfield shift of 0.1 ppm (Figure S8, the Supporting Information). Complexes **2** and **3** displayed additional peaks in the region 1.0-2.0 ppm which were due to the aliphatic protons of the ammine groups chelated to platinum(II). An intense signal was also observed at 3.9 ppm corresponding to the protons of two methoxy groups present in the curcumin ligand. In contrast, complex **4** displayed peaks at 1.9 ppm which were duly assigned to the aliphatic protons of the methyl group of acetylacetonate (Figure S9, the Supporting Information). Complexes **1-3** showed a broad signal at 4.5 ppm for the ammine/amine protons. The ¹³C NMR spectra of the complexes **1-3** displayed peaks for the aromatic carbons in the range 110-150 ppm (Figures S10-S12, the Supporting Information). The signals corresponding to the carbonyl and methyl carbons appeared at 175 and 55 ppm, respectively. For complex **4**, aliphatic carbons appeared at 23 ppm (Figure S13, the Supporting Information). Prominent IR signals at 3200, 1590 and 1495 cm⁻¹ corresponding to N-H, C=O and C=C stretching frequencies were found for all the complexes (Figure S14, the Supporting Information). The cyclic voltammograms of the complexes **1-3** in DMF-0.1 M tetrabutylammonium perchlorate (TBAP) exhibited an irreversible redox response at -1.35 V vs.

S.C.E. (Figure S15, the Supporting Information). A similar redox peak was found in free curcumin at -1.80 V. Such redox peaks were absent in the cyclic voltammogram of complex **4** done under identical conditions. Thus this electrochemical response was assigned to reductions involving the curcumin unit.^[38] The absence of any metal based redox activity indicates the electrochemical stability of these platinum(II)-curcumin conjugates. The purity of the isolated complexes was confirmed from ICP-MS (solution phase) and CHN (solid phase) data. The absorption spectra of the complexes **1-3** recorded in 10% DMSO-DPBS (Dulbecco's phosphate-buffered saline, pH, 7.2) displayed broad intense absorption band at 450 nm ($\epsilon = 2.25 \times 10^4 \text{ M}^{-1} \text{ cm}^{-1}$) which was similar to that of free curcumin (Figure 2a). The acac analogue, **4**, showed only a weak absorption at 380 nm ($\epsilon = 0.55 \times 10^4 \text{ M}^{-1} \text{ cm}^{-1}$) implying the necessity of curcumin to observe strong absorptions in the visible region. The curcumin conjugates **1-3** of platinum were emissive in 1:1 aq. DMSO with a characteristic unstructured band at 530 nm ($\lambda_{\text{ex}} = 430 \text{ nm}$). The calculated fluorescence quantum yield (Φ_f) values were in the range 0.01-0.02. The emission intensity of curcumin was quenched in the complexes when compared to free curcumin ($\Phi_f = 0.04$). This loss in emission intensity was attributed to the presence of platinum (Figure 2b).^[36d]

X-ray crystallography

Complex **4** having CF₃SO₃ as a counter ion (**4a**) was characterized by X-ray crystallography. Complex **4a** crystallized in the orthorhombic Cmc2₁ space group with four molecules in the unit cell (Figure 3c,d). Selected crystallographic and bonding parameters are given in Tables 2 and 3. The data are consistent with those from the previously reported crystal structures of β -diketonate complexes of platinum(II).^[39-41] The structure revealed the Pt(II) centre in a distorted square-planar geometry with two NH₃ ligands and a chelating monoanionic acac. The Pt-O and Pt-N bond lengths are 1.990(6) and 2.046(8) Å, respectively. In the unit cell packing diagram, it was observed that the adjacent O atom of (CF₃SO₃) and N atom (of NH₃) are ~2.5 Å apart from each other which resulted in extensive hydrogen bonding interactions stabilizing four molecules in the unit cell (Figure 3d).

Stability studies in dark and light

The stability of complexes **1-4** was studied in 10% DMSO-DPBS or DMEM (Dulbecco's modified eagle medium, pH = 7.2, 37 °C) by monitoring UV-visible spectral changes with time. Complexes **1-3** showed slow hydrolysis as compared to the curcumin dye alone. Curcumin degraded rapidly and only ~10% remained intact in 4 h, while complexes **1-3** were ~75% intact (Figure S16, the Supporting Information).^[36] This indicates improved stability of the β -diketonate moiety on complex formation. No noticeable change in the ¹H NMR spectra of the complexes **1-3** in 1:1 D₂O:d₄-MeOD even after 48 h further suggested their enhanced stability. Slow release of the ligands in a cellular medium is well documented for platinum conjugates of O,O-

For internal use, please do not delete. Submitted_Manuscript

donor ligands.^[3,5,27] Few reports also indicate probable photo-triggered ligand loss from the platinum(II) centre.^[42-46] Both curcumin and platinum(II) complexes are known for their excellent photophysical properties. The conjugation of curcumin with a heavy metal like platinum further amplifies the possibilities of photo-dissociation of complexes **1-3**. This made us curious to investigate the possibility of release of the dye on exposure to light (Luzchem, 400-700 nm) and in the dark. Photoexposure of complexes **1-3** in 1:1 DMSO-water solutions led to a gradual enhancement of emission intensity at 530 nm (Figure 4a, Figure S17, the Supporting Information). However, the intensity remained unchanged in darkness for 24 h indicating the necessity of light for metal-O, O-donor ligand bond dissociation.

The leaching out of curcumin was further supported by fluorescence lifetime measurements. In 1:1 aqueous DMSO, complexes **1-3** gave the respective fluorescence lifetime values of 13.6, 12.5 and 10.2 ps. After 1h light exposure (400-700 nm) of these solutions of the curcumin complexes, an increase in the lifetime values (~18-20 ps) resulted. Free curcumin showed a constant fluorescence lifetime value of 23 ps in the dark and when exposed to light. Furthermore, the absorption spectra of **1-3** when exposed to visible light resulted in a gradual loss of intensity at 460 and 435 nm with concomitant increase at 385 and 400 nm (Figure 4b, Figure S18, the Supporting Information). These bands are probably appearing due to the formation of free curcumin and its degraded products.^[47] In 10% DMSO-DPBS medium (pH, 7.2), the platinum-curcumin conjugates **1-3** displayed immediate loss of the emission and absorption intensity on short photo-exposure times of only 10 min (400-700 nm) (Figures S19, S20, the Supporting Information). The released curcumin was unstable at pH of 7.2, a degraded further into smaller organic components which led to the rapid reduction of intensity. Traces of free curcumin ($m/z = 369$, $[M+H]^+$) was observed in the mass spectral analysis of the irradiated samples of **1-3** (Figure S21, the Supporting Information). In contrast, the control complex **4** was found to be stable under photo-irradiated conditions (400-700 nm, 1h) proving that the intense visible band of curcumin at ~450 nm is important for observing light promoted degradation of the complexes **1-3**.

Interactions of platinum(II) with DNA

The light promoted Pt-O bond breakage is expected to generate Pt(II) species with two labile sites. These active species are known to interact with several nucleophiles and form stable adducts e.g. the Pt-DNA covalent crosslinks.^[1-3,5] To ascertain such possibilities, complex **1** was treated with excess of guanosine monophosphate (5'-GMP, 1:10 ratio in 1:1 D₂O-d₆DMSO) and exposed to light (400-700 nm). Platinum(II) binds to N7 position of GMP to form stable Pt-GMP adducts which is reflected in an downfield shift of the H8 proton ($\delta = 8.1$ ppm) in ¹H NMR spectra.^[48] Thus, the reaction was monitored by ¹H NMR spectra as a function of time. After 8 h of light exposure of complex **1**, new peaks appeared at 8.5 and 9.2 ppm (Figure S22, the Supporting Information). The observed downfield shift of 0.4 and 1.1 ppm of H8 proton was respectively assigned to the bi-

and mono-functional Pt-GMP adducts.^[49] Additional experiments performed using complexes **1-3**, ct-DNA (300 μ M) and ethidium bromide (EB, 50 μ M) in 5% DMSO-DPBS medium confirmed the Pt-DNA crosslink formation. EB, a standard DNA intercalator, exhibits strong emission at 595 nm ($\lambda_{\text{excitation}} = 546$ nm) in aqueous solutions only in presence of DNA. This happens because of entrapment of EB molecules in the hydrophobic core of DNA formed by the base pairs which reduces the external quenching by water molecules.^[50] The emission intensity of DNA intercalated EB (~13%) decreased in presence of complex **1** (50 μ M) and only when exposed to light suggesting formation of Pt-DNA adducts (Figure S23, the Supporting Information). Addition of excess thiourea (10 mM) to this solution led to a marginal increase in the emission intensity indicating only ~2% of adducts being mono-functional.^[51] Curcumin alone did not alter the emission intensity of EB since it has no DNA intercalating properties. To rule out any intercalative displacement of EB by complexes **1-3** with ct-DNA, the DNA melting studies were performed. Complexes **1-3** and curcumin showed no DNA intercalative property ($\Delta T_m \sim 0^\circ\text{C}$) as compared to EB ($\Delta T_m \sim 19^\circ\text{C}$) (Figure 5a). Interestingly, complexes **1-3** on light exposure gave similar temperature shifts as cisplatin in the dark ($\Delta T_m \sim 1.0^\circ\text{C}$). The higher melting points of the complexes **1-3** (~150 $^\circ\text{C}$) ensured their thermal stability at 100 $^\circ\text{C}$ during DNA melting experiments. Thus the degradation of the complexes was solely triggered by light in the DNA melting studies. The non-intercalative nature of the platinum(II) curcumin analogues **1-3** was also evident from DNA viscosity studies (Figure 5b). The stepwise addition of the complexes (25 μ M) showed minor change in viscosity of ct-DNA (200 μ M) which was similar to that of classical groove binder Hoechst dye. The acac analogue, **4** was exceptionally photo-stable and exhibited no enhanced Pt-DNA adducts formation on long exposure to visible light (400-700 nm).

Theoretical studies

Computational studies were carried out using Becke 3-Parameter (Exchange), Lee, Yang and Parr (B3LYP) functional with basis sets LanL2DZ for Pt/6-31+G* for C,H,N,O with Gaussian 09 programs to rationalize the photophysical properties of the complexes **1-4**.^[52-54] The initial coordinates for the coordination sphere were adapted from the crystal structure of complex **4a**. The entire structure was then modified by adding fragments as required. These coordinates were subjected to DFT calculations to obtain the energy-minimized structures (Figures 3b, S24, Table S1, the Supporting Information) of the complexes. The HOMO of the complexes **1-3** resides mainly on the curcumin moiety while the LUMO comprises of orbitals on both the curcumin unit and platinum(II) metal. Further TDDFT calculations revealed the dipole allowed transitions in the visible region along with the oscillator strengths. Few selected transitions along with the nature of orbitals and their contributions are given in Table S2 (vide Supporting Information). All the three curcumin complexes showed a strong LMCT band near 490 nm ($f \sim 0.8$) which corresponded to the dissociative ¹LMCT: HOMO (Hcur) \rightarrow LUMO (Pt-O bond) (Figures 6 a,b, S25,

For internal use, please do not delete. Submitted_Manuscript

the Supporting Information). The presence of heavy metals like platinum results in spin-orbit coupling which is likely to enhance intersystem crossing (ISC) and population of long-lived triplet states.^[55,56] Thus we optimized the triplet state of complex **1** to gain additional insights on structural changes of the photo-excited molecule. The triplet excited state geometry revealed elongation of Pt-O bonds by ~ 0.2 Å with substantial puckering of the planar curcumin moiety (C1-C2-C3-C4 dihedral angle of 26°) (Figure S26, the Supporting Information). A decrease in the respective Mulliken charges on Pt and O was also observed in the computed excited state (Table S3, the Supporting Information). This geometrical perturbation creates excessive strain in the photo-excited molecule which may lead to elimination of curcumin. TDDFT calculations performed on complex **4** revealed weak absorptions only at higher energies (328 and 288 nm) which agree with its spectral properties observed by experimental methods.

Photocytotoxicity studies

The observed formation of curcumin and a DNA crosslinking agent on light exposure prompted us to assess the light mediated anticancer potency of **1-3** and free curcumin. The standard MTT, [3-(4,5-dimethylthiazol-2-yl)-2,5-diphenyltetrazolium bromide], assay^[57] was employed to obtain the IC_{50} values in the dark and light conditions in various human cell lines, viz. HaCaT (immortalized transformed skin keratinocytes), BT474 and T47D (breast epithelial ductal carcinoma) and Hep3B (hepatocarcinoma) cells (Figure 7, Table 4, Figures S27, S28, the Supporting Information). The basic principle is the reduction of MTT to insoluble violet formazan in presence of reducing enzymes of viable cells. Thus the spectroscopically detected amount of formazan directly correlates with the number of viable cells. A human normal cell line, HPL1D (immortalized non-transformed human peripheral lung epithelial) was taken to evaluate the extent of selective activity of these complexes in cancer cells. The cells were incubated with different concentrations of the complexes or the ligand for 4 h in the dark and then subjected to irradiation with visible light for 1 h (400-700 nm, 10 J cm^{-2}). It was observed that the platinum complexes of curcumin displayed superior solubility in 1% DMSO-DMEM of up to $220 \mu\text{M}$, while free curcumin was soluble only up to a concentration of $50 \mu\text{M}$. Complex **1** was found to be the most potent of all the complexes showing IC_{50} values of $12 - 18 \mu\text{M}$ in light, while being relatively non-toxic in the dark [$IC_{50} > 200 \mu\text{M}$]. The IC_{50} values of **1** in light were comparable to that of free curcumin ($10 - 13 \mu\text{M}$) under similar conditions. Complex **1** showed about two-fold lower photocytotoxicity [IC_{50} (light) $\sim 30 \mu\text{M}$] in HPL1D cells as compared to the cancer cells. This is attributed to the inherent higher cellular uptake of the cancer cells as compared to normal cells due to their abnormal elevated metabolic rates. Complexes **2** and **3** were found to be less active giving IC_{50} values of $35-60 \mu\text{M}$ in light. One possible reason for the low photocytotoxicity can be their low cellular uptake. Moreover, it is known that the hydrogen atoms of the ammine group play important role in preferential selection of DNA as target by the platinum(II) moiety

in comparison to other proteins or sulphur nucleophiles.^[58] Additionally, the presence of rigid bidentate amine donors such as ethylenediamine (en) in **2** or 1,2-diaminocyclohexane (dach) in **3** reduces the flexibility which in turn results in less efficient Pt-DNA adduct formation.^[59] The acac complex **4** gave similar IC_{50} values in dark and light (within $80 - 180 \mu\text{M}$) showing no pronounced PDT activity due to its inability to act as a photosensitizer in the visible region.

DCFDA assay and DNA photocleavage studies

2',7'-Dichlorofluorescein diacetate (DCFDA) assay was done to detect the generation of reactive oxygen species (ROS) in HaCaT cells after incubation with the complexes **1-3** and curcumin for 4 h followed by either irradiation with visible light (400-700 nm) or kept in the dark.^[60] Cells treated with the complexes **1-3** and exposed to light (400-700 nm, 10 J cm^{-2}) showed pronounced DCF fluorescence intensity as compared to those kept in dark which was indicated by the shift in the band (Figure S29, the Supporting Information). To elucidate the nature of ROS, the DNA photocleavage experiments were conducted with complexes **1-3** using pUC19 DNA and various ROS quenchers (Figure 8). The irradiation wavelength of 457 nm was chosen based on the absorption maxima of the complexes **1-3** at 450 nm. Complexes **1-3** ($10 \mu\text{M}$ in buffer having 10% DMF, pH 7.2) resulted in $\sim 90\%$ of the nicked circular (NC) formation on laser irradiation. The presence of singlet oxygen quenchers like NaN_3 and TEMP diminished the amount of the NC form by $\sim 25\%$. Addition of hydroxyl radical scavengers (KI and DMSO) displayed marked reduction ($\sim 50\%$ NC) in the DNA photocleavage activity suggesting that hydroxyl radicals are the major ROS. The DNA cleavage was reduced ($\sim 20\%$ NC) in an inert atmosphere implying the need of aerial oxygen for its photoactivity.

Cellular Apoptosis

The annexin-V/FITC assay was performed in HaCaT cells treated with the complexes **1-3** for 4 h in dark followed by 1 h irradiation with visible light (400-700 nm).^[61] Complexes **1-3** caused early apoptotic cell death in nearly $80 - 85\%$ of the total cell population (Figures 9, S30, the Supporting Information) when irradiated with visible light but there was no significant cell death observed in the dark ($10-15\%$ early apoptotic population). Curcumin under analogous conditions resulted in late apoptotic cell death (80%). The photoinactive complex **4** induced early apoptotic features in only 8% of the HaCaT cells in dark and light which were similar to that of untreated cells kept as controls (Figure S32, the Supporting Information).

The propidium iodide based cell cycle assay was studied in HaCaT cells alone or in presence of the complexes **1-3** with and without irradiation by FACS analysis. In contrast, the photo-active complexes, **1-3** induced much higher sub-G1 population ($50 - 60\%$) in HaCaT cells upon exposure to light (400-700 nm). The complexes failed to hinder the cell cycle progression when

For internal use, please do not delete. Submitted_Manuscript

kept in dark. Untreated cells or cells treated with complex **4** did not alter the cell cycle progression in both light and dark.

Fluorescence microscopy

To monitor the exact subcellular co-localization of the fluorescent complexes **1-3** inside HaCaT cells, we carried out fluorescence microscopic experiments with several tracker dyes. The images of the tracker (red channel) when overlapped with the images of the complex **1** (green channel) revealed the cellular localization of the complex. Merged images revealed the cytoplasmic accumulation of complex **1** (Figure 10). The complex however showed a diffused distribution throughout the cytoplasm indicating non-specific localization of the complex in mitochondria, endoplasmic reticulum as well as the lysosomes. Complexes **2** and **3** did not show any emission signals in HaCaT cells probably due to their low cellular uptake as compared to complex **1**.

Cytoplasmic localization of platinum(II) complexes are more desired since it asserts direct damage on cellular metabolism compelling the cell to collapse. The predominant accumulation of complex **1** in cytoplasmic organelles motivated us to further investigate the probable release of active platinum(II) species which might migrate to different cellular targets. To deduce the exact mechanism, we conducted fluorescence microscopic experiments in HaCaT cells in presence of light. Complex **1** was located even after 4h suggesting its stability, while free curcumin degraded with no apparent fluorescence after 2h in dark (Figure S31, the Supporting Information). This proved the enhanced stability of curcumin in the platinum bound form. However, on light exposure, the apparent increase in fluorescence intensity indicated detachment of curcumin from the platinum(II) centre (Figure S32, the Supporting Information).

Estimation of cellular Pt content

The fate of the platinum(II) moiety in cellular medium was determined with the help of platinum estimation by ICP-MS method. HaCaT cells were treated with complex **1** (50 μM) in both light (400-700 nm, 30 min) and dark conditions and the nuclear and cytoplasmic fractions were separated using known procedures. Pt estimation in isolated nuclear and cytoplasmic fractions by ICP-MS confirmed that complex **1** essentially remained in the cytoplasm in the dark (2.1 $\mu\text{g}/10^6$ cells) (Table S4, the Supporting Information). The same experiment with additional 30 min of visible light exposure resulted in a substantial platinum content in both nuclear (1.68 $\mu\text{g}/10^6$ cells) and cytoplasmic (1.46 $\mu\text{g}/10^6$ cells) extracts. This indicates that the active Pt(II) species is probably migrating from the cytosol to its conventional target, the nuclear DNA.^[1-3,58] The total cellular platinum quantification studies also revealed that complex **1** showed higher cellular uptake than complexes **2** and **3** which might be attributed to its higher photocytotoxicity. Complex **1** also showed better cellular accumulation than complex **4** or cisplatin probably due to lipophilicity of curcumin.

Comet assay

To examine the formation of Pt-DNA crosslinks by complex **1**, we additionally performed the comet assay using HaCaT cells (Figure S33, S34, the Supporting Information).^[62,63] The formation of interstrand and intrastrand crosslinks stabilizes duplex DNA and hence reduces the % DNA content in the tail region. Complex **1** (15 μM) showed only ~30% DNA content in tail region of the photo-exposed cells (400-700 nm). Untreated cells displayed ~90% of DNA in the comet tail. The behaviour of complex **1** in light was analogous to that of cisplatin (200 μM in the dark) indicating similar type of Pt-DNA crosslink formation.

Conclusions

We have synthesized platinum(II) complexes of curcumin and characterized them using elaborate techniques. Herein, we have shown that these complexes can act as prodrugs for delivering the two potential anticancer agents, viz. curcumin and a reactive cisplatin species, specifically in the cancer cells which can be monitored by visible light. Unformulated curcumin degrades rapidly in a biological medium thus resulting its poor bioavailability. On the other hand, the lability of cisplatin generates non-specific interactions enroute to targeted tumors. Thus a controlled activation of both curcumin and cisplatin specifically in cancerous tissues can overcome the associated drawbacks of the individual drugs. Complex **1** exhibited photo-degradation on visible light exposure which was evident from various spectral and analytical studies. This unique property led to the controlled generation of diammineplatinum(II) species as a DNA crosslinking agent and the released curcumin as a potential photosensitizer. The phototoxic profile of complex **1** was found to be the most potent in the series of investigated complexes ($\text{IC}_{50} \sim 12\text{-}18 \mu\text{M}$, 400-700 nm light). The complex also showed at ~15 fold lower dark toxicity which is an essential feature of the PDT agents. Complexes **2** and **3** were less photocytotoxic ($\text{IC}_{50} \sim 35 \mu\text{M}$, 400-700 nm light) probably due to reduced cellular uptake and the presence of rigid $\text{N}^{\wedge}\text{N}$ donors. Thus minor modifications in the structures can have a profound impact on the visible light activated dual-action anticancer properties of these complexes. Future works need to be directed towards their rational design for improved stability, selectivity and efficacy as light promoted platinum-based anticancer agents.

Experimental Section

Materials and Methods: Potassium tetrachloroplatinate and cisplatin were purchased from Arora Matthey, India. All other chemicals were purchased from Sigma Aldrich, USA. Curcumin was used as purchased without any further purification. The purchased solvents were dried by well established protocols before using them for synthesis and other experiments. The cellular reagents were obtained from Sigma Aldrich or Invitrogen, USA.

Elemental analysis was conducted using Thermo Finnigan Flash EA 1112 CHNS analyzer. Electrospray ionization mass spectrometry (ESI-

For internal use, please do not delete. Submitted_Manuscript

MS) was carried out using Agilent 6538 Ultra High Definition (UHD) Accurate Mass-Q-TOF (LC-HRMS) instrument. ^1H and ^{13}C NMR spectra were recorded in Bruker 400 MHz NMR spectrometer. The infrared, UV-visible and emission spectra were obtained from Bruker Alpha, Perkin Elmer and Spectrum 750 spectrophotometer, Perkin Elmer LS 55 spectrophotometer respectively. A Control Dynamics (India) conductivity meter was used to measure the molar conductivity of the complexes. EG&G PAR Model 253 VersaStat potentiostat/galvanostat combined with electrochemical analysis software 270 and equipped with a three electrode setup (glassy carbon working electrode, a platinum wire auxiliary electrode and a saturated calomel electrode (SCE) as reference) was used for performing the electrochemical studies. Tetrabutylammonium perchlorate (TBAP, 0.1 M) was used as a supporting electrolyte. The ICP-MS data for the platinum content was obtained from ICP-MS, Thermo X, series II. All the experiments with light irradiation was done using a Luzchem Photoreactor (Model LZC-1, Ontario, Canada) fitted with 8 fluorescent Sylvania white tubes. MTT assay data were obtained from Molecular Devices Spectra Max M5 plate reader. Fluorescence assorted cell sorting experiments were done using FACS Verse instrument (BD Biosciences). Fluorescence microscopy images were acquired using Olympus 1X 80 fluorimeter with oil immersion lens having magnification of 63X.

Synthesis: The complexes were synthesized using modified methods as reported earlier.^[39,40] The precursor complexes $[\text{Pt}(\text{en})\text{Cl}_2]$ and $[\text{Pt}(\text{dach})\text{Cl}_2]$ were prepared using reported synthetic procedures.

Syntheses of the complexes 1-4

The precursor complex cisplatin (0.25 g, 0.84 mmol) for **1** and **4**, $[\text{Pt}(\text{en})\text{Cl}_2]$ (0.28 g, 0.84 mmol) for **2**, $[\text{Pt}(\text{dach})\text{Cl}_2]$ (0.32 g, 0.84 mmol) for **3** was taken in 5 mL of DMF or water and treated with two equivalents of AgNO_3 (0.27 g, 1.63 mmol). The solution was stirred at room temperature for 12 h in dark and then filtered. The yellowish filtrate was drop-wise added to the respective deprotonated 1,3-diketone solution, prepared by adding Na_2CO_3 (0.103 g, 1.00 mmol) to curcumin (0.307 g, 0.84 mmol) for **1-3** or acac (0.085 g, 0.84 mmol) for **4**, and the reaction was continued for 5 h in the dark at room temperature under nitrogen atmosphere (Schemes S1, S2, the Supporting Information). The solution was then filtered and DMF or water was evaporated using rotovac at an elevated temperature. The red oil thus obtained was re-dissolved in little volume of DMF. Diethyl ether (100 mL) was added to it and allowed to stand for 30 min in ice-cold condition. The resulting bright yellow precipitate was filtered and washed with diethyl ether and water and dried. Complex **4a** was synthesized using a similar procedure as for complex **4** by treating with AgCF_3SO_3 instead of AgNO_3 and was used solely for the purpose of crystallization.

[Pt(NH₃)₂(cur)](NO₃) (1): Yield, ~51% (280 mg, 0.425 mmol). Anal. Calcd for $\text{C}_{21}\text{H}_{25}\text{N}_3\text{O}_9\text{Pt}$ [Mw: 658.53]: C, 38.30; H, 3.83; N, 6.38. Found: C, 38.18; H, 3.95; N, 6.13. ESI-MS in MeOH: m/z (observed) = 596.13 $[\text{M} - \text{NO}_3]^+$ (100%). ^1H NMR (400 MHz, MeOD-*d*₄): δ (ppm) = 7.65 (d, J = 16 Hz, 2H), 7.21 (d, J = 1.2 Hz, 2H), 7.11 (m, 2H), 6.80 (d, J = 8.4 Hz, 2H), 6.55 (d, J = 15.6 Hz, 2H), 5.88 (s, 1H), 3.91 (s, 6H). ^{13}C NMR (100 MHz, MeOD-*d*₄): δ (ppm) = 176.13, 174.97, 149.10, 148.56, 140.47, 128.31, 122.71, 115.71, 110.39, 55.48. UV-visible in 10% DMSO-DPBS (pH = 7.2) $[\lambda_{\text{max}}$, nm (ϵ , M⁻¹ cm⁻¹): 453 (2.24 × 10⁴), 437 (2.24 × 10⁴). IR data in solid phase (cm⁻¹): 3200 br, 1590 s, 1509 s, 1345 m (br, broad; s, strong; m, medium). Λ_{M} (S m² M⁻¹) in 50% aq. DMSO at 25 °C: 80.

[Pt(en)(cur)](NO₃) (2): Yield, ~50% (0.28 g, 0.44 mmol). Anal. Calcd for $\text{C}_{23}\text{H}_{27}\text{N}_3\text{O}_9\text{Pt}$ [Mw: 684.56]: C, 40.35; H, 3.98; N, 6.14. Found: C, 40.15; H, 3.95; N, 6.10. ESI-MS in MeOH: m/z (observed) = 622.15 $[\text{M} - \text{NO}_3]^+$ (100%). ^1H NMR (400 MHz, MeOD-*d*₄): δ (ppm) = 7.52-7.50 (m, 2H),

7.27-7.21 (m, 2H), 7.17-7.11 (m, 2H), 6.88-6.84 (m, 2H), 6.70-6.60 (m, 2H), 5.93 (s, 1H), 3.95 (s, 6H), 1.22 (t, J₁ = 8 Hz, J₂ = 4 Hz, 4H). ^{13}C NMR (100 MHz, MeOD-*d*₄): δ (ppm) = 175.13, 148.61, 140.18, 126.22, 122.79, 115.75, 110.36, 65.10, 55.54. UV-visible in 10% DMSO-DPBS (pH = 7.2) $[\lambda_{\text{max}}$, nm (ϵ , M⁻¹ cm⁻¹): 450 (1.5 × 10⁴), 430 (1.5 × 10⁴). IR data in solid phase (cm⁻¹): 3215 br, 1592 s, 1512 s, 1342 m. Λ_{M} (S m² M⁻¹) in 50% aq. DMSO at 25 °C: 71.

[Pt(dach)(cur)](NO₃) (3): Yield, ~50% (0.28 g, 0.42 mmol). Anal. Calcd for $\text{C}_{27}\text{H}_{33}\text{N}_3\text{O}_9\text{Pt}$ [Mw: 738.65]: C, 43.90; H, 4.50; N, 5.69. Found: C, 43.75; H, 4.65; N, 5.70. ESI-MS in MeOH: m/z (observed) = 677.20 $[\text{M} - \text{NO}_3]^+$ (100%). ^1H NMR (400 MHz, MeOD-*d*₄): δ (ppm) = 7.60-7.55 (m, 2H), 7.24-7.21 (m, 2H), 7.11-7.06 (m, 2H), 6.85-6.80 (m, 2H), 6.67-6.60 (m, 2H), 5.88 (s, 1H), 3.93 (s, 6H), 1.623-1.61 (b, 4H), 1.30-1.19 (b, 4H). ^{13}C NMR (100 MHz, MeOD-*d*₄): δ (ppm) = 177.25, 175.03, 149.61, 148.62, 148.51, 140.14, 127.61, 123.20, 122.91, 115.64, 110.72, 63.00, 24.61. UV-visible in 10% DMSO-DPBS (pH = 7.2) $[\lambda_{\text{max}}$, nm (ϵ , M⁻¹ cm⁻¹): 450 (1.45 × 10⁴), 430 (1.38 × 10⁴). IR data in solid phase (cm⁻¹): 3200 br, 1588 s, 1525 s, 1345 m. Λ_{M} (S m² M⁻¹) in 50% aq. DMSO at 25 °C: 79.

[Pt(NH₃)₂(acac)](NO₃) (4): Yield, ~45% (0.150 g, 0.33 mmol). Anal. Calcd for $\text{C}_5\text{H}_{13}\text{N}_3\text{O}_5\text{Pt}$ [Mw: 390.26]: C, 15.39; H, 3.36; N, 10.77. Found: C, 15.10; H, 3.53; N, 10.58. ESI-MS in MeOH: m/z (observed) = 328.0565 $[\text{M} - \text{NO}_3]^+$ (100%). ^1H NMR (400 MHz, MeOD-*d*₄): δ (ppm) = 5.61 (s, 1H), 1.87 (s, 6H). ^{13}C NMR (100 MHz, MeOD-*d*₄): δ (ppm) = 184.70, 102.19, 24.88. UV-visible in 10% DMSO-DPBS (pH = 7.2) $[\lambda_{\text{max}}$, nm (ϵ , M⁻¹ cm⁻¹): 308 (5540), 272 (4720). IR data in solid phase (cm⁻¹): 3250 br, 1560 w, 1525 w, 1300 s (w, weak). Λ_{M} (S m² M⁻¹) in 50% aq. DMSO at 25 °C: 75.

X-ray Crystallographic Procedures

The crystal structure of $[\text{Pt}(\text{NH}_3)_2(\text{acac})](\text{CF}_3\text{SO}_3)$ (**4a**) was obtained by single crystal X-ray diffraction method. Yellow colored crystals of **4a** were obtained on slow evaporation of a methanol solution of the complex. The crystal was mounted on a loop with paratone oil. All geometric and intensity data were collected using an automated Bruker SMART APEX CCD diffractometer equipped with a fine focus 1.75 kW sealed tube Mo-K α X-ray source ($\lambda = 0.71073$ Å) with increasing ω (width of 0.3° per frame) at a scan speed of 5 sec per frame. Intensity data were collected using the ω -2 θ scan mode and then corrected for the Lorentz-polarization and absorption effects.^[64] The structure was solved and refined using the WinGx suite of programs (Version 1.63.04a) by the SHELXL-2013 method.^[65] The non-hydrogen atoms were refined with anisotropic displacements coefficients and their coordinates were permitted to ride on their respective carbon atoms. The perspective view of complex **4a** in the crystallographic asymmetric unit is presented using ORTEP.^[66] CCDC number is 1415424. It contains the supplementary crystallographic data for this structure. These data can be obtained free of charge from The Cambridge Crystallographic Data Centre

Fluorescence Lifetime Measurements

Fluorescence lifetimes of complex **1** and curcumin (50 μM in 50% aq. DMSO solutions) were measured using HORIBA Jobin Yvon IBH fluorescence spectrometer. Samples were either kept in the dark or irradiated with visible light (400-700 nm, 10 J cm⁻²) and the fluorescence lifetimes were recorded. The fluorescence intensity followed either tri-exponential decay of complex **1** or double-exponential decay for curcumin [depending on value of goodness of fit (χ^2) ~ 1]. The lifetime value having the highest pre-exponential fitting factor denotes the lifetime of the molecule.

For internal use, please do not delete. Submitted_Manuscript

Experiments with EB and ct-DNA

Ethidium bromide (EB) intercalated to calf thymus (ct) DNA is trapped in a hydrophobic environment created by the base pairs and exhibits fluorescence which is otherwise quenched in DNA free aqueous solutions. However, in presence of a DNA crosslinking agent, the fluorescence intensity of EB decreases due to partial displacement. The fluorescence spectra of EB (50 μM) intercalated to ct-DNA (300 μM) was recorded ($\lambda_{\text{ex}} = 546 \text{ nm}$, $\lambda_{\text{em}} = 595 \text{ nm}$) in presence of the complexes (**1-4**) or curcumin (50 μM in 5% DMSO-DPBS, pH = 7.2) in the dark and under photo-irradiated conditions (400-700 nm, 10 J cm^{-2}). Thiourea is known to hinder the formation of lethal crosslinks by reacting with cis-Pt(II) DNA monoadducts. However, it cannot reverse the reaction once the crosslinks have been formed. Therefore, to assess the amount of Pt-DNA monofunctional adducts, the solutions were further treated with excess of thiourea (10 mM) and the emission spectra were recorded. Decrease in emission intensity can be quantitatively correlated with the amount of monofunctional adducts.

DNA Melting Experiments

At higher temperatures, DNA strands break and exhibits hyperchromicity at 260 nm. The melting temperature of DNA (T_m) is defined as the temperature where 50% of the DNA is denatured. In presence of the intercalators, ds-DNA gets stabilized and it melts at higher temperature as compared to groove or surface binders or crosslinking agents. The DNA thermal denaturation experiments were done by measuring the absorption intensity of ct-DNA (230 μM) at 260 nm at elevated temperatures (from 40 to 90 $^{\circ}\text{C}$), both in the absence and presence of the compounds (24 μM in 1% DMSO-DPBS solutions, pH = 7.2). EB (24 μM), a standard intercalator was used for comparison. Experiments were also carried out using ct-DNA, complexes **1** and visible light (400-700 nm, 5 J cm^{-2}). Calf thymus (ct) DNA alone was irradiated as a positive control for the experiment. Almost similar values of T_m of DNA alone in dark and light ensured that no significant DNA damage occurred due to light exposure.

DNA Viscosity Experiments

Viscosity measurements were carried out to confirm the non-intercalative nature of complexes **1-4** and curcumin. ct-DNA (200 μM) was treated with varying concentrations of the compounds using [complex]/[DNA] ratio in the range of 0.0-0.4 in DPBS at pH = 7.2.

Platinum Estimation in ct-DNA

The ct-DNA (200 μM) was treated with complexes **1-3** (50 μM in 1% DMSO-DPBS) in duplicates. One set was exposed to broadband white light (400-700 nm) immediately after addition, while the other was kept in the dark. Samples were then treated with 10 mL of ethanol to precipitate the platinated-DNA from buffer solutions. The precipitate was then collected by centrifuging (12000 g at 4 $^{\circ}\text{C}$) and washed repeatedly with ethanol to remove any unbound free platinum salts. The precipitates were dissolved in 10 mL of 2% HNO_3 solutions and estimated for platinum by ICP-MS method along with the untreated samples as control and standard platinum solutions for calibration. The experiment, each done in duplicates, was repeated twice.

Theoretical Study

The geometries of the complexes **1-4** were optimized by density functional theory (DFT) using B3LYP level of theory [LanL2DZ (for Pt atom)/6-31+G (for all other atoms)] with Gaussian 09 suites programs.⁵²

⁵⁴ The coordinates for the basic framework involving the metal coordination sphere of complexes **1-3** were adapted from the crystal structure of complex **4a** and then the fragment added as required by using Chemcraft software. These coordinates were used to obtain the energy minimized structure of **1-4**. TDDFT calculations done on the energy-minimized structures of these complexes gave the electronic transitions along with the oscillator strengths. The triplet state of complex **1** was optimized in a similar way and the bond-lengths, bond-angles and Mulliken charges were obtained from the output files.

DNA Photocleavage Experiments

The cleavage of supercoiled (SC) pUC19 DNA (0.2 μg , 30 μM , 2686 base-pairs) in the presence of the **1-3** and Hcur (10 μM in 10% DMF-50 mM Tris-HCl buffer containing 50 mM NaCl, pH 7.2) was determined by agarose gel electrophoresis. The photo-induced DNA cleavage reactions were done using Ar-Kr mixed gas ion monochromatic CW laser (Spectra Physics, power = 50 mW) of 457 nm based on the absorption spectral band at $\sim 450 \text{ nm}$ of the complex and curcumin. The observed DNA cleavage was expressed as % of nicked-circular (NC) DNA. The mechanistic investigations were done by adding different additives as singlet oxygen quenchers (NaN_3 and TEMP, 4 mM) and hydroxyl radical scavengers (DMSO, 8 μL ; KI, 4 mM).

MTT Assay and other Cellular Studies: Cytotoxicity studies were done using complexes **1-4** in HaCaT (immortalized transformed human skin keratinocytes), BT474 and T47D (human breast epithelial ductal carcinoma), Hep3B (human hepatocarcinoma), HPL1D (immortalized non-transformed human peripheral lung epithelial cells). Cells were incubated with various concentrations of **1-4** [200, 100, 75, 50, 25, 12.5, 6.25, 3.125 μM dissolved in 1% DMSO-DMEM] for 4 h in complete darkness. One set of cells was exposed to visible light (400 – 700 nm, 10 J cm^{-2}), while the other was kept in the dark for 1 h. Data were obtained using three independent sets of experiments done in triplicates for each concentration. Details of MTT assay and other cellular assay are provided in the Supporting Information.

Acknowledgements

A.R.C. thanks the Department of Science and Technology (DST), Government of India, for providing financial support (SR/S5/MBD-02/2015, EMR/2015/000742). A.R.C. also thanks the DST for J. C. Bose fellowship. P.K. Acknowledges financial support from the DBT-IISc partnership program. We thank Alexander von Humboldt Foundation, Germany, for an electrochemical system. K.M. thanks BMS for fellowship. We acknowledge the use of FACS and microscopy facility of IISc. We thank Dr. R. Chakrabarti from the department of CEaS, IISc for the ICP-MS facility.

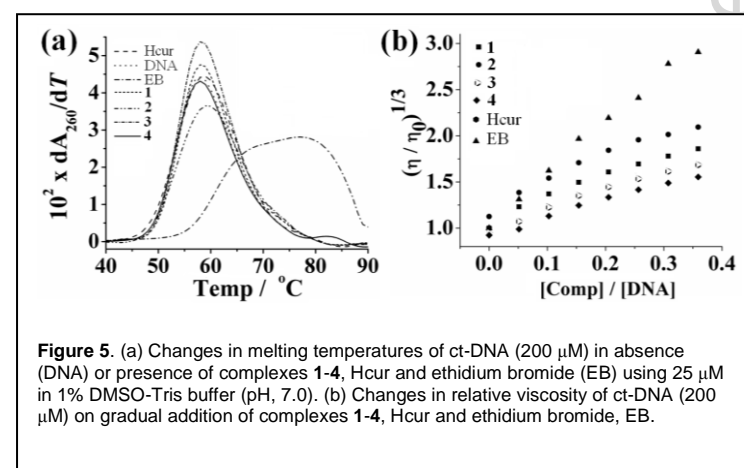
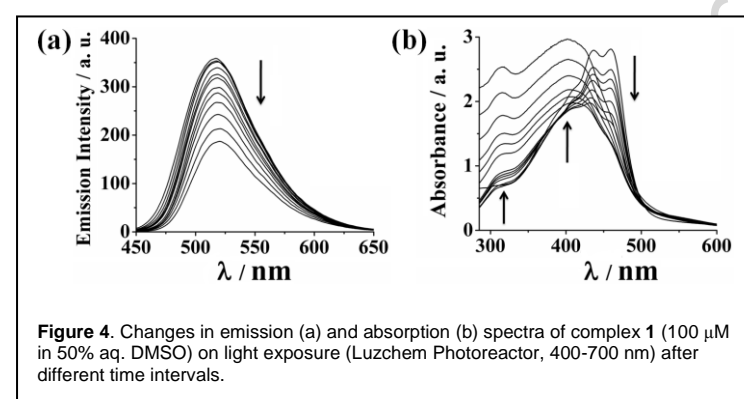
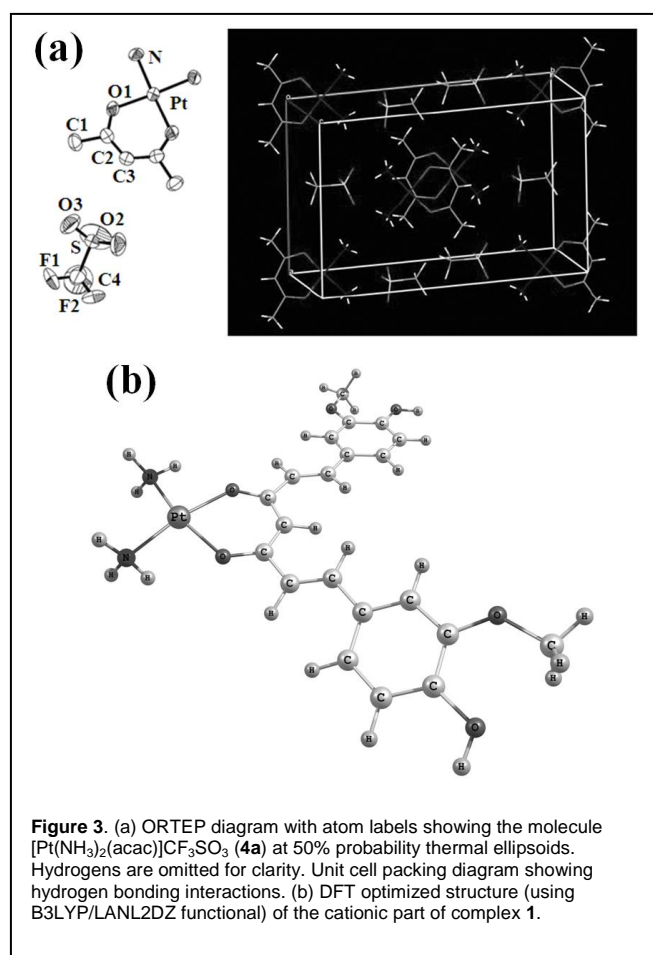
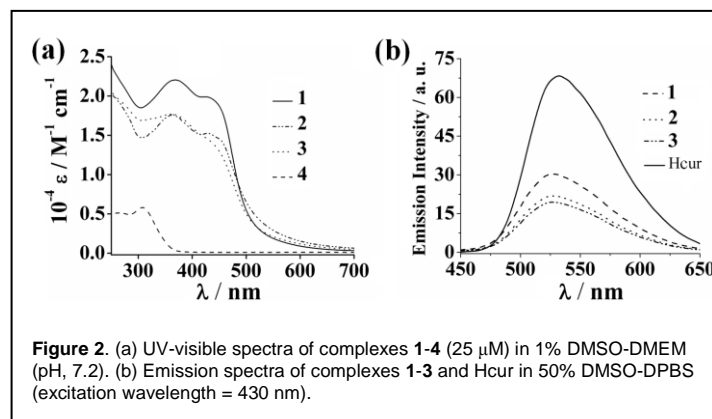
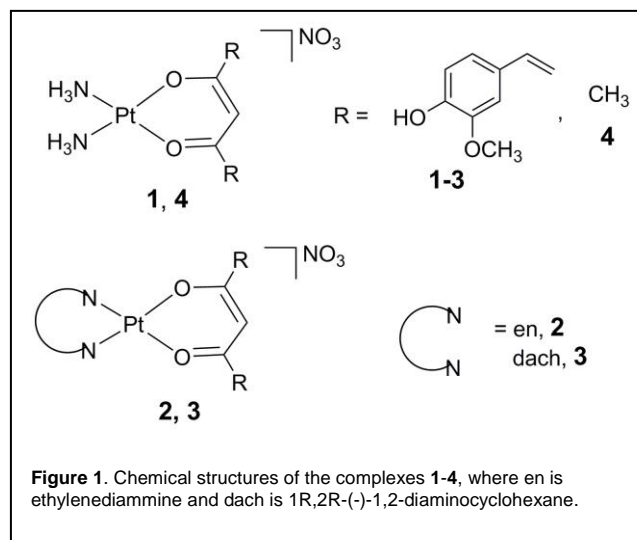
Keywords: platinum • curcumin • DNA crosslinking • bioinorganic chemistry • cytotoxicity

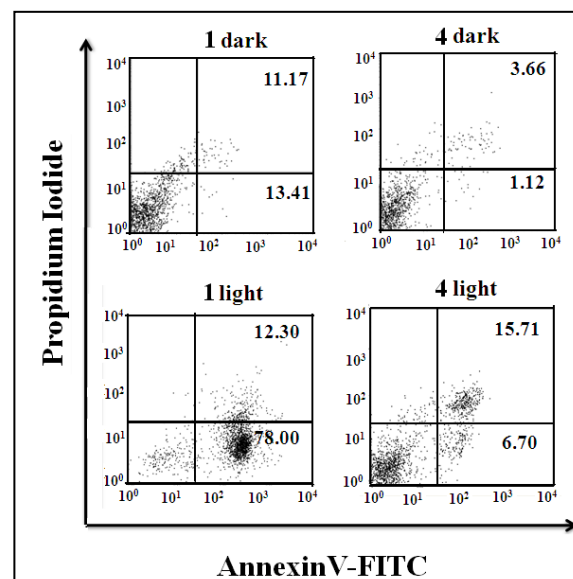
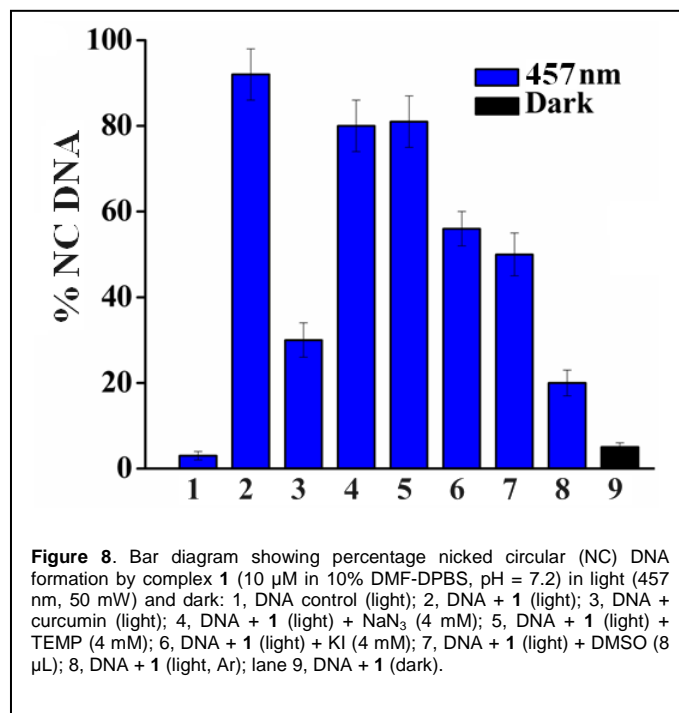
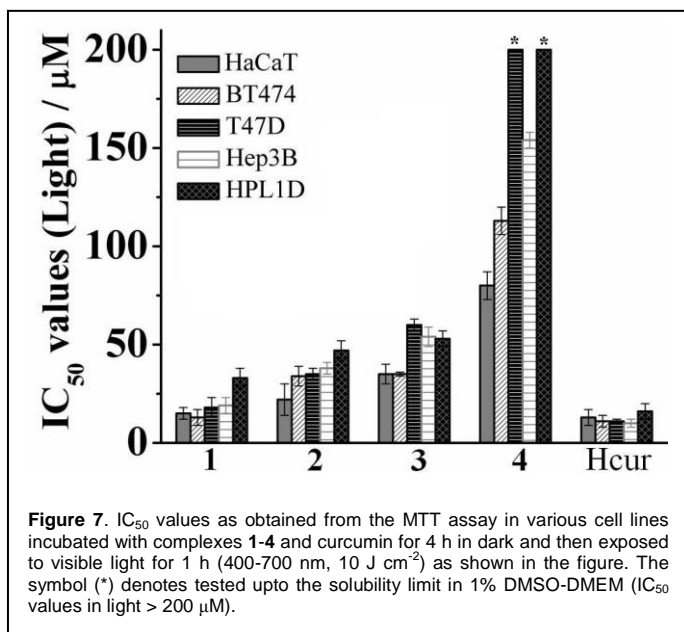
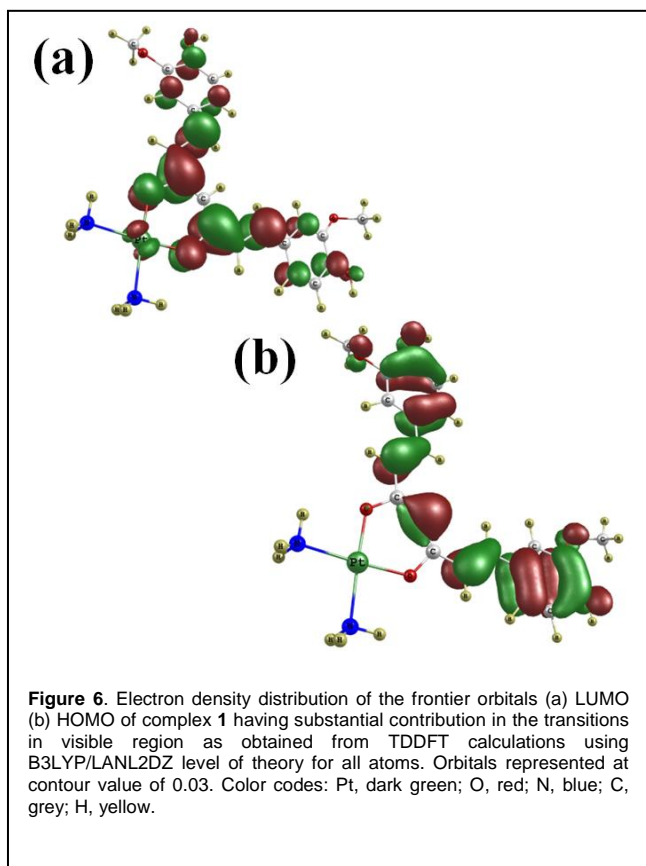
- [1] a) T. C. Johnstone, K. Suntharalingam, S. J. Lippard, *Chem. Rev.* **2016**, 116, 3436-3486. b) S. Dilruba, G. V. Kalayda, *Cancer Chemother. Pharmacol.* **2016**, 77, 110324.
- [2] Q.-Q. Deng, X.-E. Huang, L.-H. Ye, Y.-Y. Lu, Y. Liang, J. Xiang, *Asian Pac. J. Cancer Prev.* **2013**, 14, 413-417.
- [3] A. M. Florea, D. Büsselberg, *Cancers* **2011**, 3, 1351-1371.
- [4] A. V. Klein, T. W. Hambley, *Chem. Rev.* **2009**, 109, 4911-4920.

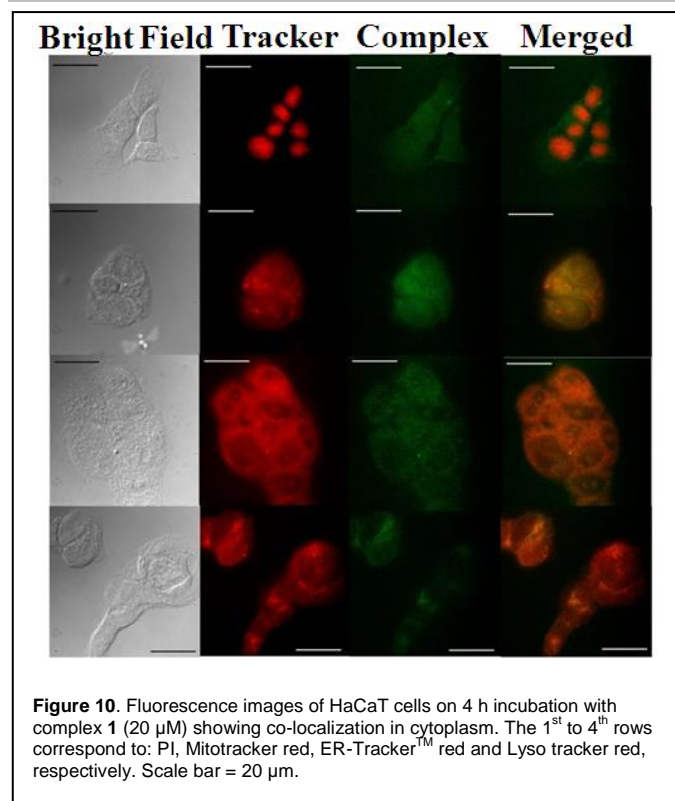
For internal use, please do not delete. Submitted_Manuscript

- [5] D. Gibson, *Dalton Trans.* **2009**, 10681-10689.
- [6] Ž. D. Bugarčić, J. Bogojeski, B. Petrović, S. Hochreutherb, R. Eldik, *Dalton Trans.* **2012**, 41, 12329-12345.
- [7] S. Amptoulach, N. Tsavaris, *Chemother. Res. Pract.* **2011**; 2011: 843019.
- [8] V. Hellberg, I. Wallin, S. Eriksson, E. Hernlund, E. Jerremalm, M. Berndtsson, S. Eksborg, E. S. J. Arnér, M. Shoshan, H. Ehrsson, G. Laurell, *J. Natl. Cancer Inst.* **2009**, 101, 37-47.
- [9] N. P. Farrell, *Chem Soc. Rev.* **2015**, 44, 8773-8775.
- [10] T. C. Johnstone, G. Y. Park, S. J. Lippard, *Anticancer Res.* **2014**, 34, 471-476.
- [11] N. J. Wheate, S. Walker, G. E. Craig, R. Oun, *Dalton Trans.* **2010**, 39, 8113-8127.
- [12] X. Wang, X. Wang, Z. Guo, *Acc. Chem. Res.* **2015**, 48, 2622-2631.
- [13] X. Han, J. Sun, Y. Wang, Z. He, *Med. Res. Rev.* **2015**, 35, 1268-1299.
- [14] J. J. Wilson, S. J. Lippard, *Chem. Rev.* **2014**, 114, 4470-4495.
- [15] S. Dhar, S. J. Lippard, *Proc. Natl. Sci. Acad. USA*, **2009**, 106, 22199-22204.
- [16] Y.-R. Zheng, K. Suntharalingam, T. C. Johnstone, H. Yoo, W. Lin, J. G. Brooks, S. J. Lippard, *J. Am. Chem. Soc.* **2014**, 136, 8790-8798.
- [17] R. K. Pathak, S. Marrache, J. H. Choi, T. B. Berding, S. Dhar, *Angew. Chem. Int. Ed.* **2014**, 53, 1963-1967.
- [18] K. Suntharalingam, Y. Song, S. J. Lippard, *Chem. Commun.* **2014**, 50, 2465-2467.
- [19] L. Ronconi, P. J. Sadler, *Dalton Trans.* **2011**, 40, 262-268.
- [20] Y. Zhao, J. A. Woods, Nicola J. Farrer, K. S. Robinson, J. Pracharova, J. Kasparkova, O. Novakova, H. Li, L. Salassa, A. M. Pizarro, G. J. Clarkson, L. Song, V. Brabec, P. J. Sadler, *Chem. Eur. J.* **2013**, 19, 9578-9591.
- [21] J. S. Butler, J. A. Woods, N. J. Farrer, M. E. Newton, P. J. Sadler, *J. Am. Chem. Soc.* **2012**, 134, 16508-16511.
- [22] Y. Zhao, N. J. Farrer, H. Li, J. S. butler, R. J. McQuitty, A. Habtemariam, F. Wang, P. J. Sadler, *Angew. Chem. Int. Ed.* **2015**, 54, 14478-14482.
- [23] P. Müller, B. Schröder, J. A. Parkinson, N. A. Kratochwil, R. A. Coxall, A. Parkin, S. Parsons, P. J. Sadler, *Angew. Chem. Int. Ed.* **2003**, 42, 335-339.
- [24] (a) E. Shaili, *Sci. Prog.* **2014**, 97, 20-40. (b) J. D. Knoll, C. Turro, *Coord. Chem. Rev.* **2015**, 282-283, 110-126.
- [25] B. S. Howerton, D. K. Heidary, E. C. Glazer, *J. Am. Chem. Soc.* **2012**, 134, 8324-8327.
- [26] Bonnet R. *Metal Complexes for Photodynamic Therapy*, In: J. A. McCleverty, T. J. Meyer, editors. *Comprehensive Coord. Chem. II*. **2004**, 9, Elsevier, Oxford, 945-1003.
- [27] (a) K. Mitra, S. Patil, P. Kondaiah, A. R. Chakravarty, *Inorg. Chem.* **2015**, 54, 253-264. (b) K. Mitra, A. Shettar, P. Kondaiah, A. R. Chakravarty, *Inorg. Chem.* **2016**, 55, 5612-5622.
- [28] T. Esatbeyoglu, P. Huebbe, I. M. A. Ernst, D. Chin, A. E. Wagner, G. Rimbach, *Angew. Chem. Int. Ed.* **2012**, 51, 5308-5332.
- [29] M. Salem, S. Rohani, E. R. Gillies, *RSC Adv.* **2014**, 4, 10815-10829.
- [30] S. Prasad, A. K. Tyagi, B. B. Aggarwal, *Cancer Res. Treat.* **2014**, 46, 2-18.
- [31] I. K. Priyadarsini, *J. Photochem. Photobiol. C Photochem. Rev.* **2009**, 10, 81-95.
- [32] a) Wanninger, S.; Lorenz, V.; Subhan, A.; Edelmann, F. T. *Chem. Soc. Rev.* **2015**, 44, 4986-5002. b) M. Pröhl, U. S. Schubert, W. Weigand, M. Gottschaldt, *Coord. Chem. Rev.* **2016**, 307, 32-41.
- [33] Pettinari, R.; Marchetti, F.; Pettinari, C.; Condello, F.; Petri, A.; Scopelliti, R.; Riedel, T.; Dyson, P. J. *Dalton Trans.* **2015**, 44, 20523-20531.
- [34] a) Renfrew, A. K.; Bryce, N. S.; Hambley, T. W. *Chem. Sci.* **2013**, 4, 3731-3739. b) Renfrew, A. K.; Bryce, N. S.; Hambley, T. W. *Chem. Eur. J.* **2015**, 21, 15224-15234.
- [36] a) S. Banerjee, A. R. Chakravarty, *Acc. Chem. Res.* **2015**, 48, 2075-2083. b) A. Bhattacharyya, A., A. Dixit, K. Mitra, S. Banerjee, A. A. Karande, A. R. Chakravarty, *Med. Chem. Commun.* **2015**, 6, 846-851.
- c) P. Prasad, I. Pant, I. Khan, P. Kondaiah, A. R. Chakravarty, *Eur. J. Inorg. Chem.* **2014**, 2420-2431. d) K. Mitra, S. Gautam, P. Kondaiah, A. R. Chakravarty, *Angew. Chem.* **2015**, 54, 13989-13993.
- [37] a) W. Scarano, P. de Souza, M. H. Stenzel, *Biomater. Sci.* **2015**, 3, 163-174. b) H. Zhang, T. Yu, L. Wen, H. Wang, D. Fei, C. Jin, *Exp. Ther. Med.* **2013**, 6, 1317-1321. c) Notarbartolo, M.; Poma, P.; Perri, D.; Dusonchet, L.; Cervello, M.; D'Alessandro N. *Cancer Lett.* **2005**, 224, 53-65. d) V. M. Duarte, E. Han, M. S. Veena, A. Salvado, J. D. Suh, L. J. Liang, K. F. Faull, E. S. Srivatsan, M. B. Wang, *Mol. Cancer Ther.* **2010**, 10, 2665-2675. e) N. M. Yunos, P. Beale, J. Q. Yu, F. Huq, *Anticancer Res.* **2011**, 31, 1131-1140.
- [38] K. Li, Y. Li, L. Yang, L. Wang, B. Ye, *Anal. Methods*, **2014**, 6, 7801-7808.
- [39] J. J. Wilson, S. J. Lippard, *J. Med. Chem.* **2012**, 55, 5326-5336.
- [40] H. Yuge, T. K. Miyamoto, *Acta Crystallogr. Sect. C.* **1997**, 53, 1816-1819.
- [41] S. Roy, I. Hartenbach, B. Sarkar, *Eur. J. Inorg. Chem.* **2009**, 2553-2558.
- [42] K. L. Ciesinski, L. M. Hyman, D. T. Yang, K. L. Haas, M. G. Dickens, R. J. Holbrook, K. J. Franz, *Eur. J. Inorg. Chem.* **2010**, 2224-2228.
- [43] Y. Zhao, G. M. Roberts, S. E. Greenough, N. J. Farrer, M. J. Paterson, W. H. Powell, V. G. Stavros, P. J. Sadler, *Angew. Chem. Int. Ed.* **2012**, 51, 11263-11266.
- [44] A. Presa, R. F. Brissos, A. B. Caballero, I. Borilovic, L. Korrodi-Gregório, R. Pérez-Tomás, O. Roubeau, P. Gamez, *Angew. Chem. Int. Ed.* **2015**, 54, 4561-4565.
- [45] P. Heringova; J. Woods, F. S. Mackay, J. Kasparkova, P. J. Sadler, V. Brabec, *J. Med. Chem.* **2006**, 49, 7792-7798.
- [46] A. Naik, R. Rubbiani, G. Gasser, B. Spingler, *Angew. Chem. Int. Ed.* **2014**, 53, 6938-6941.
- [47] U. Singh, S. Verma, H. N. Ghosh, M. C. Rath, K. I. Priyadarsini, A. Sharma, K. K. Pushpa, S. K. Sarkar, T. Mukherjee, *J. Mol. Catal. A: Chem.* **2010**, 318, 106-111.
- [48] A. T. M. Marcellis, C. G. van Kralingen, J. Reedijk, *J. Inorg. Biol. Chem.* **1980**, 13, 213-222.
- [49] T. N. Singh, C. Turro, *Inorg. Chem.* **2004**, 43, 7260-7262.
- [50] S. P. Sau, P. Kumar, P. W. Sharma, P. J. Hrdlicka, *Nucleic Acids Res.* **2012**, 1-9.
- [51] A. Eastman, M. A. Barry, *Biochemistry* **1987**, 26, 3303-3307.
- [52] M. J. Frisch, et al., GAUSSIAN 09, Revision D.01, *Gaussian, Inc., Wallingford CT 2009* (see Supporting Information for full reference).
- [53] A. D. Becke, *Phys. Rev. A* **1998**, 38, 3098-3100.
- [54] A. D. Becke, *J. Chem. Phys.* **1993**, 98, 5648-5652.
- [55] L. Salassa, H. I. A. Phillips, P. J. Sadler, *Phys. Chem. Chem. Phys.* **2009**, 11, 10311-10316.
- [56] M. Pope, C. Swenberg, *Electronic Processes in Organic Crystals; Clarendon Press: Oxford*, **1982**.
- [57] T. Mosmann, *J. Immunol. Methods*, **1983**, 65, 55-63.
- [58] J. Reedijk, *Chem Rev.* **1999**, 99, 2499-2510.
- [59] H. Cui, R. Goddard, K.-R. Pörschke, A. Hamacher, M. U. Kassack, *Inorg. Chem.* **2014**, 53, 3371-3384.
- [60] M. Price, D. Kessel, *J. Biomed. Opt.* **2010**, 15, 516051-516053.
- [61] I. Vermes, C. Haanen, H. Stefens-Nakken, C. Reutelingsperger, *J. Immunol. Methods* **1995**, 184, 39-51.
- [62] O. Merck, G. Speit, *Environ. Mol. Mutagen.* **1999**, 33, 167-172.
- [63] S. Pfuhler, H. U. Wolf, *Environ. Mol. Mutagen.* **1996**, 27, 196-201.
- [64] N. Walker, D. Stuart, *Acta Crystallogr. Sect. A* **1983**, A39, 158-166.
- [65] G. M. Sheldrick, *Acta Crystallogr. Sect. A* **2008**, 64, 112-122.
- [66] C. K. Johnson, *ORTEP, Report ORNL-5138*; Oak Ridge National Laboratory: Oak Ridge, TN, **1976**.

For internal use, please do not delete. Submitted_Manuscript





**Table 2.** Selected crystallographic data for complex **4a**

Empirical formula	C ₁₆ H ₁₃ F ₃ Pt N ₂ O ₅ S
FW	477.32
Crystal System	Orthorhombic
Space Group	Cmc2 ₁
a (Å)	11.3355(4)
b (Å)	17.5357(6)
c (Å)	6.7178(2)
V (Å ³)	1474.7(7)
Z	4
2θ _{max} / °C	51.0
T (K)	293 (2)
ρ _{calcd} (g cm ⁻³)	2.374
λ (Å) (Mo K _α)	0.71073
μ (mm ⁻¹)	10.713
Data/ restraints/ parameters	1312 / 1 / 88
F(000)	896.0
Goodness of fit	1.441
R (F _o) ^a , I > 2σ(I) / wR (F _o) ^b	0.0311/ 0.0788
R (all data) / wR (all data)	0.0346/ 0.0769
largest diff. peak and hole (e Å ⁻³)	1.157, -2.263

$$^a R = \sum ||F_o| - |F_c|| / \sum |F_o|. \quad ^b wR = \{ \sum [w(F_o^2 - F_c^2)^2] / \sum [w(F_o^2)] \}^{1/2}. \\ w = [\sigma^2(F_o)^2 + (AP)^2 + BP]^{-1}, \text{ where } P = (F_o^2 + 2F_c^2)/3.$$

Table 1. Selected physicochemical data of the complexes **1-4** and curcumin (Hcur)

Complex	δ / ppm ^a	λ _{abs} /nm (10 ⁻⁴ ε / M ⁻¹ cm ⁻¹) ^b	λ _{em} /nm (Φ) ^c	IR (NO ₃ ⁻) ^d /cm ⁻¹	Λ _M ^e /S m ² M ⁻¹	E _r ^f /V
1	5.88	460 (2.25), 435 (2.25)	525 (0.02)	1509, 1345	80	-1.35
2	5.93	450 (1.5), 430 (1.5)	520 (0.01)	1512, 1342	71	-1.30
3	5.88	450 (1.45), 430 (1.38)	520 (0.01)	1509, 1345	79	-1.30
4	5.61	308 (0.55), 272 (0.47)	--	1525, 1300	75	--
Hcur	5.99	430 (2.45), 358 (1.52)	530 (0.04)	--	--	-1.80

^a ¹H NMR chemical shift of the methylene proton in d₄-MeOD. ^b In 10% DMSO-DPBS solutions (pH, 7.2). ^c In 1:1 aq. DMSO solutions. Excitation wavelength is 430 nm. Quantum yield is measured by taking pure fluorescein as standard (Φ = 0.79). ^d In solid phase. ^e Molar conductivity values in 1:1 aq. DMF at 25 °C. ^f Peaks observed in cyclic voltammograms (1mM complexes in DMF-0.1 M TBAP) represented vs. SCE at a scan rate of 100 mV s⁻¹.

Table 3. Selected bond lengths and bond angles of complex **4a**

Bond	Bond Length /Å	Bond	Bond Angle /°
Pt - O(1)	1.990(6)	O(1) - Pt - O(1)'	95.8(3)
Pt - N(1)	2.046(8)	O(1) - Pt - N(1)	89.6(3)
O(1) - C(2)	1.280(9)	C(2) - O(1) - Pt	121.7(5)
C(1) - C(2)	1.504(11)	O(1) - C(2) - C(3)	126.9(8)
C(2) - C(3)	1.392(10)	O(1) - C(2) - C(1)	113.5(7)

Table 4. IC₅₀ values (in μM) of complexes **1-4** in various cell lines ^a

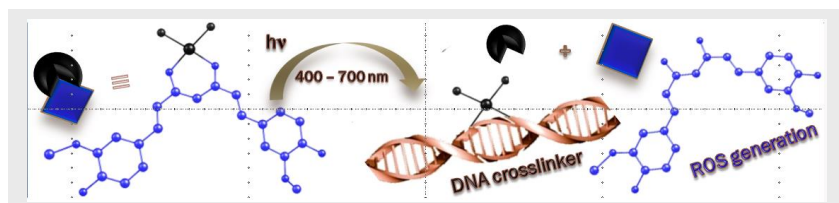
Cell Types	1	2	3	4	Hcur
HaCaT, skin keratinocytes	15 ± 3 (>200)	22 ± 8 (>200)	35 ± 5 (>200)	80 ± 7 (90 ± 5)	13 ± 4 (38 ± 2)
BT474, breast epithelial carcinoma	13 ± 4 (>200)	34 ± 5 (>200)	35 ± 1 (>200)	113 ± 7 (137 ± 7)	11 ± 3 (>50)
T47D, breast epithelial carcinoma	18 ± 5 (>200)	35 ± 3 (>200)	60 ± 3 (>200)	>200 (>200)	11 ± 1 (>50)
Hep3B, hepato-carcinoma	19 ± 4 (>200)	38 ± 3 (>200)	54 ± 5 (>200)	184 ± 4 (>200)	10 ± 2 (>50)
HPL1D, normal human epithelial cells	33 ± 5 (>200)	47 ± 5 (>200)	53 ± 4 (>200)	>200 (>200)	16 ± 4 (>50)

^a The IC₅₀ values in μM correspond to cells incubated with compounds for 4h and then exposed to visible light for 1h (400-700 nm, 10 J cm⁻²). The values in parenthesis are the IC₅₀ values in μM of identical samples kept in dark. Data are obtained from three independent sets of experiments, each performed in duplicates.

Entry for the Table of Contents (Please choose one layout)

Layout 2:

FULL PAPER



Platinum(II) curcumin complexes having diammine or chelating amines as ligands show photocytotoxicity in visible light with dissociation of curcumin ligand generating platinum(II) DNA crosslinking agents and curcumin as phototoxin.

Koushambi Mitra,^[a] Srishti Gautam,^[b]
Paturu Kondaiah^{✉[b]} and Akhil R.
Chakravarty^{✉[a]}

Page No. – Page No.

**Platinum(II) complexes of curcumin
showing photocytotoxicity in visible
light**

Accepted Manuscript